Welding in the World (2023) 67:585–592
https://doi.org/10.1007/s40194-022-01405-2

RESEARCH PAPER

Comparative analysis of CoCrAlY coatings at high-temperature oxidation behavior using different reinforcement composition profiles

H. S. Nithin[1] · K. M. Nishchitha[2] · D. G. Pradeep[1,3] · C Prasad Durga[4] · Mahantayya Mathapati[5]

Received: 31 May 2022 / Accepted: 27 October 2022 / Published online: 7 November 2022

Abstract
The oxidation behaviour of plasma-sprayed carbides and oxides reinforced composite CoCrAlY coatings at 700 °C was examined in this paper. CoCrAlY was reinforced with Al_2O_3 + YSZ, CeO_2, WC–Co, Cr_3C_2-NiCr individually to produce four different coatings. SEM, EDS, and XRD are used to analyse the oxide scales formed during the oxidation process on the surface of the coating. From the results, it is found that all of these coatings had a parabolic weight gain, suggesting the existence of a shielding oxide scale on the surface, whereas changes in total weight gain are observed. The oxidation resistance of CoCrAlY + Al_2O_3 + YSZ coating is better and exhibits 28% less weight gain than other coatings. During oxidation, coating shows slow scale growth of kinetics due to thermodynamically stable Al_2O_3. The CoCrAlY + 2% CeO_2 coating showed the lowest oxidation resistance of all the coatings.

Keywords Plasma spray · CoCrAlY · Carbides · Oxides · High-temperature oxidation

1 Introduction

High-temperature applications like boiler components are commonly used in power plant sectors, and these are subjected to extreme working conditions; it could be circulation of high pressure fluid/water or steam, reaction from sulphur element presence in coal [1, 2]. The component may undergo surface degradations in the form of erosion, oxidation, hot corrosion, and wear [3, 4]. Boilers are recognised as one of the severe challenges in the course application, and development of the boiler using right combination of materials is in wide scope [5–7]. Oxidation is a major material degradation mechanism that occurs mostly in high-temperature situations such as IC engines, jet engine components, gas turbines, coal pipelines, and offshore oil [8–10]. Oxidation of alloys reduces ductility, tensile strength, corrosion, and erosion properties. Currently, nickel-based super alloys having excellent high-temperature strength are being used to manufacture the above mentioned components. However, theses alloys exhibit poor surface properties at higher temperature [11–13]. Hence, development of coatings which could able to combat against these degradations is of high interest. Several industrial components commonly have thick coatings of MCrAlY applied by plasma spray to increase service life in an oxidising environment [1, 2]. The efforts have been made by some researchers to advance the properties of MCrAlY coatings by the addition of active elements such as Ti, Zr, Hf, Si, Ta, Ce, Ru, Ir, and Mo [6]. However, these changes are not beneficial to work against critical environment like combined oxidation, corrosion wear, and erosion. Furthermore, the MCrAlY coating is reinforced with carbides and oxides to combat against both high-temperature oxidation and wear degradations [7].

WC–Co and Cr_3C_2-NiCr are the carbide coatings added with small amount of metallic binder are used for high-temperature tribological applications. These coatings have exceptional wear resistant properties; they are not most preferable in high-temperature oxidation and corrosion environments [11]. The inclusion of metal oxide particles benefits to strengthen the high temperature coating materials, which also raises the coating's hardness and wear resistance.

Recommended for publication by Commission I - Additive Manufacturing, Surfacing, and Thermal Cutting

✉ C Prasad Durga
durgaprasi71@gmail.com

1 BGSCET, Bengaluru 560086, Karnataka, India
2 BGSIT, Adichunchanagiri University, Karnataka 57144, India
3 Malnad College of Engineering, Hassan, India
4 RVITM, Bengaluru 560076, Karnataka, India
5 KLECET, Chikodi, Karnataka 591201, India

The addition of oxide particles to high-temperature coating materials strengthens the coating and eventually increases the hardness and wear resistance [9]. Most of the research articles published associated to hard phase reinforced composite coatings focussed on tribological behaviour and phase development [12–14]. However, the studies on high-temperature oxidation behaviour of these composite coating is on mandate as these composite coatings exposed to various environment.

Hatami et al., [15] studied the oxidation behavior of 0–15% YSZ mixed (5% intervals) with CoNiCrAlY powder by HVOF technique. The result reported that coating with 5%YSZ obtained the better oxidation resistance at 1000 °C. Similarly, Ghadami et al. [16] investigated the oxidation behaviour of HVOF-sprayed CeO_2-gradient NiCrAlY coatings at 1000 °C. It is reported that functionally graded NiCrAlY coating reinforced with nano-CeO_2 had a greater oxidation resistance than the mono-layered coatings with lower oxide growth rate. The rest of due to controlling Al and O diffusion due to the formation of relatively thin, dense, and sticky Al_2O_3 oxide scale.

Hang et al. [17] investigated the elevated temperature oxidation behavior of WC-12Co and rare earth-modified WC-12Co HVOF coating. The CeO_2-modified coatings have good oxidation resistance at the temperature below 550 ℃. Whereas above 650 ℃ due to the occurrence of anomalous oxidation, the oxidation mechanism changes. Similarly, comparative oxidation studies of NiCoCrAlYSiHf and NiCoCrAlYSiHf + NiAl composite coatings were reported by Yao et al. [18] at 1100 ℃. NiCoCrAlYSiHf + NiAl composite coating exhibited good oxidation resistance with the Kp value of less than two-fifths of that for NiCoCrAlYSiHf coating during isothermal oxidation. Shi et al., [19] recently reported the elevated temperature oxidation behaviour of Ni and NiCrAlY-based composite coatings by reinforcing with TiO_2-ZnO elements. The reinforcement in the coating diffuses to the surface at 800 °C and 1000 °C.

In case of NiCrAlY composite coatings, the diffusion behaviour was slower compared to Ni-based coatings at 800 °C. Whereas, diffusion behaviour greatly increased as temperature closer to 1000 °C. Similarly, Reddy et al., [20] studied the cyclic oxidation behavior of plasma-sprayed NiCrAly coating by addition of TiO_2 and Cr_2O_3-YSZ at 700 ℃. Cr_2O_3 + YSZ-reinforced NiCrAlY coating was found to exhibit highly resistive as compared with TiO_2-reinforced NiCrAlY coating in the oxidation environment.

The comparative studies with both oxides and carbides were reported in Ref [16–20] related to the high temperature oxidation and erosion behaviour of HVOF-sprayed NiCrSiB/Al_2O_3, NiCrSiB/n-Al_2O_3 and NiCrSiB/WC–Co coatings on an SS304 steel substrate. NiCrSiB/Al_2O_3 coatings exhibits superior oxidation resistance to that of NiCrSiB/WC–Co coatings due to the presence of protective oxide layers like Cr_2O_3, Al_2O_3, $NiCr_2O_4$, and NiO. The weight gain of Al_2O_3-reinforced coating was less than that of n-Al_2O_3 and WC–Co-reinforced coatings by 43% and 51% respectively. The presence volatile oxide WO_3 in WC–Co-reinforced coatings had least oxidation resistance.

From the above discussion, it can be inferred that, the addition of oxide or carbide-reinforced coating will be beneficial for both oxidation and erosion/wear resistance. In the present investigation, attempt has been made to develop four different coatings by addition of different oxides and carbides reinforcement such as Al_2O_3, CeO_2, WC and Cr_3C_2 with CoCrAlY coating. A comparative study on cyclic oxidation behavior of these plasma-sprayed composite coatings at 700 °C have been studied and reported.

2 Materials and methods

2.1 Feedstock and spray process

Cobalt-based composite powder of CoCrAlY (23Cr-13Al-0.65Y-balCo) was added with Al_2O_3 + YSZ (28% + 2%), CeO_2 (2%), WC–Co (30%), and Cr_3C_2-NiCr (30%) exclusively to prepare coating powders (feedstock). The coating powders were subjected to mechanical mixing to blend properly. The coating powders were developed by using mechanical mixing. CoCrAlY + 28%Al_2O_3 + 2%YSZ, CoCrAlY + 2%CeO_2, CoCrAlY + WC–Co, and CoCrAlY + Cr_3C_2-NiCr coating powders were plasma sprayed over the bond coat. The reinforcement was added in weight percentage. The spraying parameters specified by the feedstock powder manufacturer were used during plasma spray deposition. METCO USA 3 MB equipment was used to conduct the coating by plasma spray technique. The detailed plasma spray parameters are listed in Table 1. Coating particle size was between − 45 + 15 µm.

2.2 Oxidation test

Plasma-sprayed CoCrAlY + Al_2O_3 + YSZ, CoCrAlY + CeO_2, CoCrAlY + WC–Co, and CoCrAlY + Cr_3C_2-NiCr coatings are subjected oxidation at 700 °C in static air for 50 cycles. At the end of each cycle, the specimens were visually examined. Thermogravimetry is a technique for studying the oxidation

Table 1 Plasma spray parameters

Parameters	Quantity
Flow rate of primary gas (argon)	40 L/min
Flow rate of secondary gas (hydrogen)	7 L/min
Spray distance	100–125 mm
Powder feed rate	60 g/min
Voltage	60 V
Current	490A

mechanism reaction rate and kinetics. XRD and SEM/EDAX methods were used to identify and investigate the structural properties of reaction products from oxidised specimens.

3 Result and discussion

The cumulative weight increase (mg/cm^2) plots of CoCrAlY + Al_2O_3 + YSZ coatings as a function of time indicated in cycles are shown in Fig. 1. Table 2 shows the total weight increase of the CoCrAlY + Al_2O_3 + YSZ, CoCrAlY + CeO_2, CoCrAlY + WC–Co, and CoCrAlY + Cr_3C_2-NiCr coatings on MDN 321 and Superni 76 alloys after 50 cycles of oxidation. To analyse oxidation kinetics, Fig. 1 presents weight growth square (mg^2/cm^4) data as a function of time. There was little difference in weight increase between the two coated alloys. The rate of weight increase of the coated alloys was faster in the early oxidation cycles, which was due to the rapid formation of active element oxides. However, oxidation and oxidising species diffusion at splat borders and open pores have caused the coating splat boundaries to oxidise. The diffusion of the oxidising species along the splat boundaries and open pores is listed in Table 2 as Kp in 10^{-10} g^{2}cm^{-4} s^{-1} for all coatings on both substrates. The parabolic rate constant value of all the coatings on both substrates is shown in Table 2 in the form of Kp in 10^{-10} g^{2}cm^{-4} s^{-1}.

3.1 Phase analysis

Figure 2 shows the XRD patterns of oxidised CoCrAlY + Al_2O_3 + YSZ-, CoCrAlY + CeO_2-, CoCrAlY + WC–Co-, and CoCrAlY + Cr_3C_2-NiCr-coated

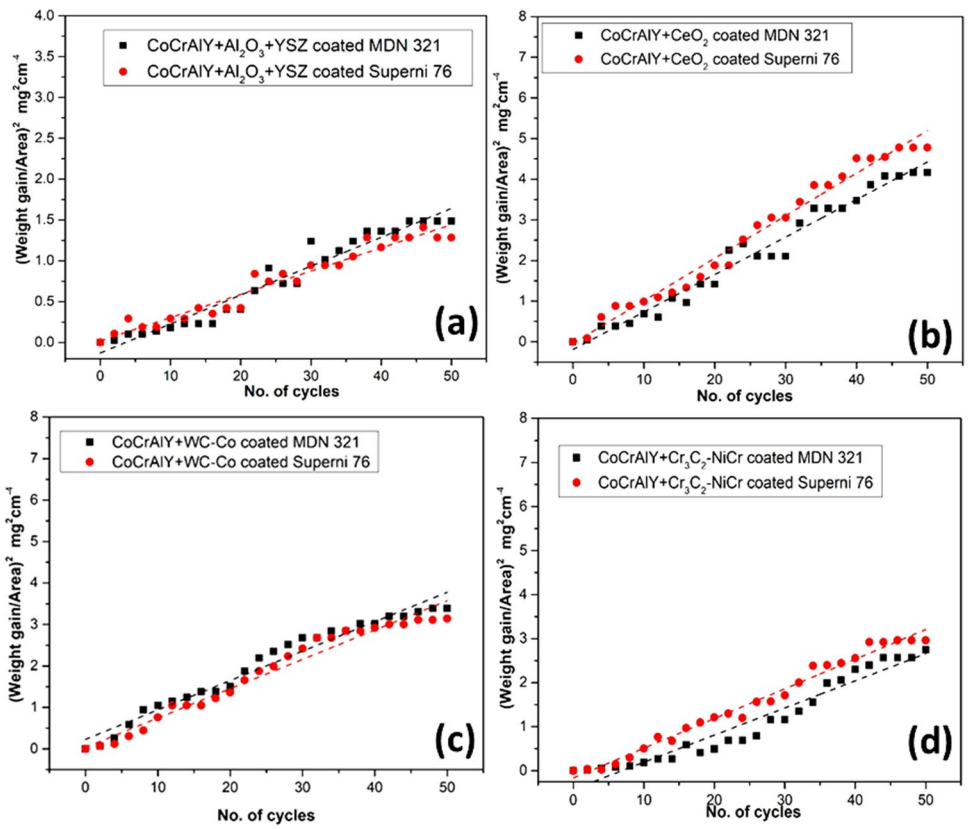

Fig. 1 (Weight gain/area)^2 vs. number of cycles plot of (**a**) CoCrAlY + Al_2O_3 + YSZ, (**b**) CoCrAlY + CeO_2, (**c**) CoCrAlY + WC–Co, and (**d**) CoCrAlY + Cr_3C_2-NiCr coatings after oxidation

Table 2 Weight gain and parabolic rate constant values of oxidised coatings

Coatings	Weight gain in mg/cm^2		Parabolic rate constant Kp in 10^{-10} g^{2}cm^{-4} s^{-1}	
	on MDN 321	on Superni 76	on MDN 321	on Superni 76
CoCrAlY + Al_2O_3 + YSZ	1.68	1.56	0.16	0.13
CoCrAlY + CeO_2	2.35	2.56	0.31	0.35
CoCrAlY + WC–Co	2.97	3.15	0.46	0.50
CoCrAlY + Cr_3C_2-NiCr	1.65	1.69	0.42	0.38

alloys at 700 °C. Cr_2O_3, CoO, $CoCr_2O_4$, and $CoAl_2O_4$ are the primary peaks of the oxidised coated alloys. Minor peaks are indexed to Al_2O_3 and AlCo respectively. The spinel oxides found in CoCrAlY + WC–Co and CoCrAlY + Cr_3C_2-NiCr coatings are $CoWO_4$ and $NiCr_2O_4$, respectively. Because the base coating composition is the same, the primary phases observed in all coatings are comparable. Furthermore, there were no peaks of elements from substrate alloys in the XRD, indicating that no diffusion from the substrate had occurred.

3.2 Coating morphologies and EDS analysis

Figure 3 a depicts the surface morphology of corroded CoCrAlY + Al_2O_3 + YSZ coatings. On the oxidised surface, bigger dark and light grey areas and spherical shapes have emerged. The existence of Co as the predominant element was discovered by EDS analysis of the dark grey area labelled region 'A' in Fig. 3a, along with nominal O and Cr and traces of Al. The light grey layer labelled area 'B' suggests that O, Cr, and Co are the most abundant elements, with traces of Al. The oxide scale CoCrAlY + CeO_2 (Fig. 3b) is made up of compact granules with peculiar dark grey patches over the oxidised coating surface. EDS examination of the dark grey patches labelled region 'A' reveals the presence of dominant Co and Cr elements with insignificant levels of Al, Ce, and O. The existence of O and Co as primary constituents, with little Cr concentration, was discovered in the compact granular structure labelled area 'B'.

Similar to CoCrAlY + Al_2O_3 + YSZ coating, the oxide scale on CoCrAlY + WC–Co indicates the presence of globular structure (Fig. 3c). Figure 3 c also shows microporous (sponge) structures with superficial fissures. The porous structure recognised the presence of W-rich oxides, which might be tungsten-trioxide (WO_3), and cracks were discovered in this defective oxide region. The surface oxide scale of the CoCrAlY + Cr_3C_2-NiCr coating (Fig. 3d) is characterised by a compact packed globular shape with patches of distributed peculiar dark grey areas over the oxidised coating surface. Globular structure is a key component of O, Cr, and Co, indicating the presence of Cr and Co oxides. Co and Ni with Al and O make up grey patches, which might suggest the existence of oxides of Co and Ni.

Figure 4 shows a SEM picture of the cross section of oxidised coatings after 50 cycles. Figure 4 b shows that all of the remaining coatings have compact, adherent oxide scale on the top surface; however, the CoCrAlY + CeO_2 coating has fissures and delamination of oxide. The EDS analysis at different places was indicated by the markings 1, 2, 3, and 4 on the cross section picture, and the corresponding elemental weight % is noted in Table 3.

3.3 Comparative discussion

In Fig. 5, the cumulative weight gain (mg/cm^2) of all oxidised coatings is indicated. When compared to the other coatings, CoCrAlY + Al_2O_3 + YSZ-coated alloys had significantly smaller weight gains. During the oxidation cycles,

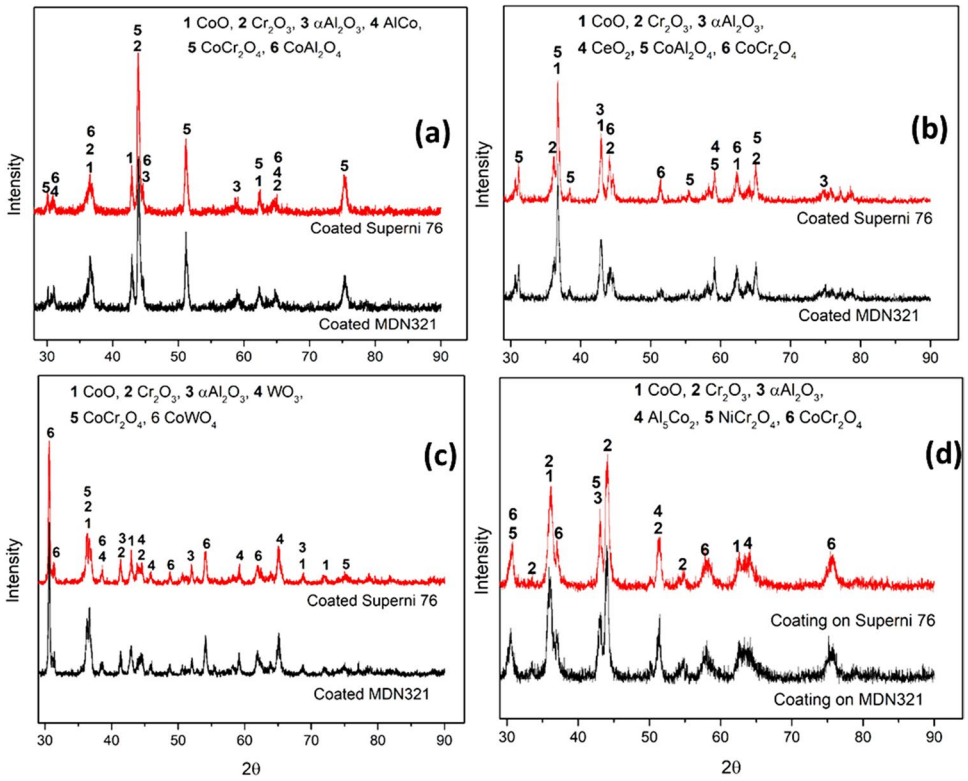

Fig. 2 XRD patterns for (**a**) CoCrAlY + Al_2O_3 + YSZ-, (**b**) CoCrAlY + CeO_2-, (**c**) CoCrAlY + WC–Co-, and (**d**) CoCrAlY + Cr_3C_2-NiCr-coated alloys subjected to oxidation

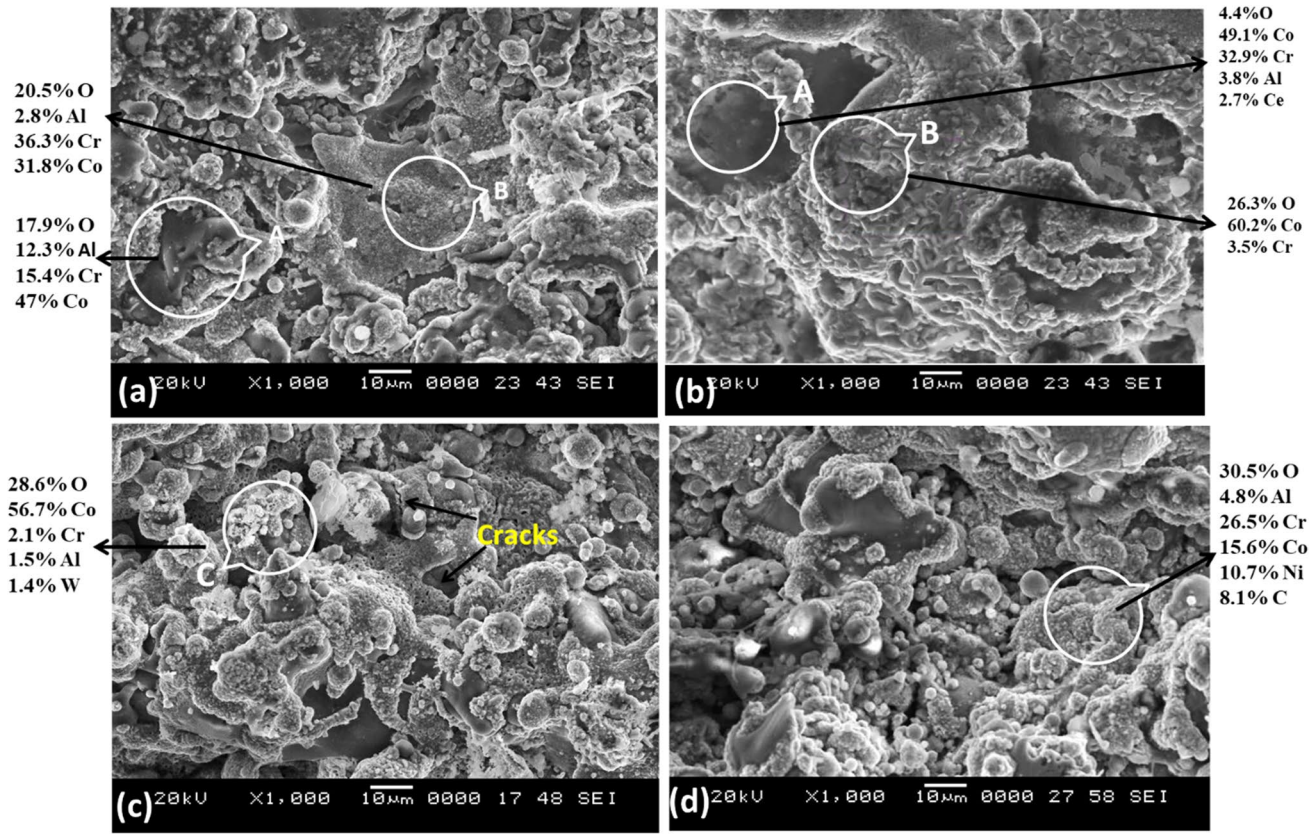

Fig. 3 Surface morphology of oxidised (**a**) CoCrAlY + Al_2O_3 + YSZ-, (**b**) CoCrAlY + CeO_2-, (**c**) CoCrAlY + WC–Co-, and (**d**) CoCrAlY + Cr_3C_2-NiCr-coated alloys subjected to oxidation

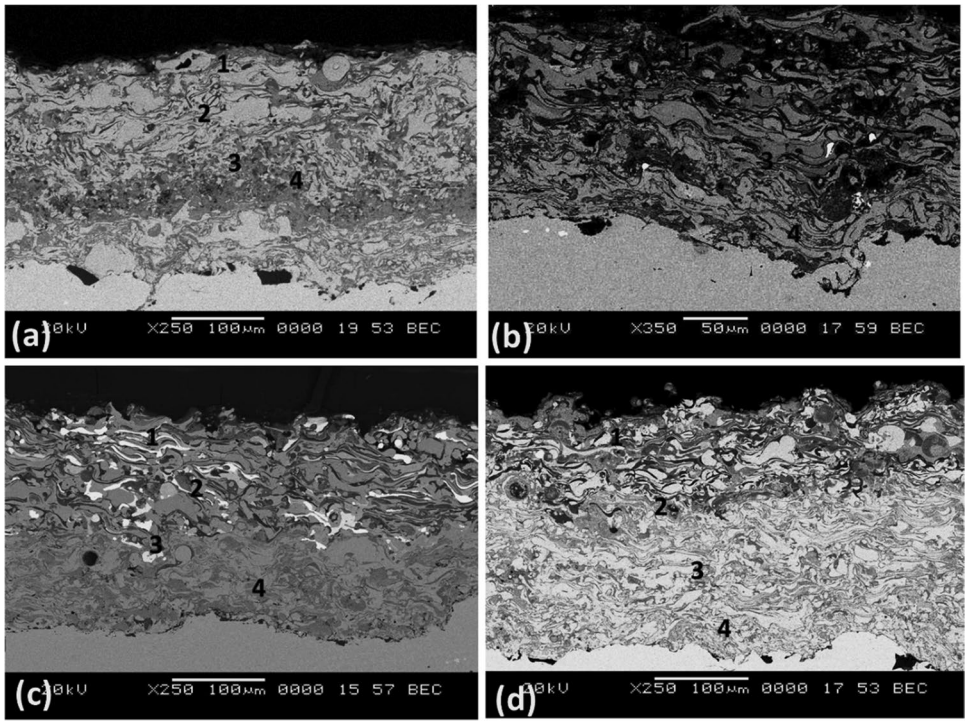

Fig. 4 Oxidised coating cross section of (**a**) CoCrAlY + Al_2O_3 + YSZ-, (**b**) CoCrAlY + CeO_2-, (c) CoCrAlY + WC–Co-, and (**d**) CoCrAlY + Cr_3C_2-NiCr-coated alloys subjected to oxidation

Table 3 EDS analysis of oxidised coatings cross section

Element (wt. %)	$CoCrAlY + Al_2O_3 + YSZ$				$CoCrAlY + CeO_2$				$CoCrAlY + WC - Co$				$CoCrAlY + Cr_3C_2$_NiCr			
	1	2	3	4	1	2	3	4	1	2	3	4	1	2	3	4
O	18.5	8.6	10	5	23.4	20.5	11	11.3	18.9	3.6	12	6.1	25.5	14.1	11.2	5.1
Al	10.8	9.7	8.1	6	2.5	9.5	7.2	10.9	5.3	-	5.9	26.8	7.5	8	15.2	2.5
Cr	47.2	18.4	17.8	14.5	14.5	13.5	12.7	17.1	11.1	1.5	10.1	17	24.6	29.5	19.2	38.2
Co	23.3	62.7	59.2	72.1	50.2	47.2	61	29.1	36.7	11.6	36.7	24.6	15.8	19.5	25.6	4.6
Ce	-	-	-	-	-	7.7	1.7	28.4	-	-	-	-	-	-	-	-
W	-	-	-	-	-	-	-	-	7	36.9	0.3	3.6	-	-	-	-
C	-	-	-	-	-	-	-	-	7	34.6	0.7	2.7	8	7.7	-	8.5
Ni	-	-	-	-	-	-	-	-	-	-	-	-	18.3	21.2	-	23.6

the parabolic weight of all of the coatings increased. Based on the data available from these cyclic oxidation trials, the sequential relative-oxidation resistance of all coatings is given in the order below:

$CoCrAlY + Al_2O_3 + YSZ > CoCrAlY + Cr_3C_2$-NiCr > Co CrAlY + WC–Co > $CoCrAlY + CeO_2$.

On the surface morphology of oxidised $CoCrAlY + Al_2O_3 + YSZ$ coating, a continuous globular with dense in structure can be seen (Fig. 4). Figure 4 a shows a thin, thick, non-porous, and well adhering oxide scale on the coating surface in a SEM image of a cross section of oxidised coating. Furthermore, the oxide scale is free of cracks. Crack-free, thin, dense, non-porous, and well adherent oxide scale are the most common topographies of protective oxides on the coated surface [21–23].

The oxygen enters minute gaps in coatings such as pores, splat boundaries, and rare voids, during the first phases of oxidation until all the accessible interior surfaces are completely oxidised. Later, the active components of the coatings Al and Cr are partly oxidised, reducing the coating's availability to supplemental oxygen. Throughout the oxidation, the distribution of thermodynamically stable Al_2O_3 in the $CoCrAlY + Al_2O_3 + YSZ$ coating underwent delayed oxide scale development kinetics [16–19]. One of the explanations for the lesser weight growth might be because the reinforcements Al_2O_3 YSZ are in a pre-oxidised phase and will not oxidise further. As a result, oxidation occurs solely on the outer surface of the coating.

The coating's basic element, Co, is oxidised to CoO, followed by Cr, which is oxidised to Cr_2O_3. With respect to $CoCrAlY + Al_2O_3 + YSZ$ coating, the oxidation of two distinct oxides leads in the creation of $CoAl_2O_4$ and $CoCr_2O_4$ spinels, which inhibits oxide development and results in a smaller

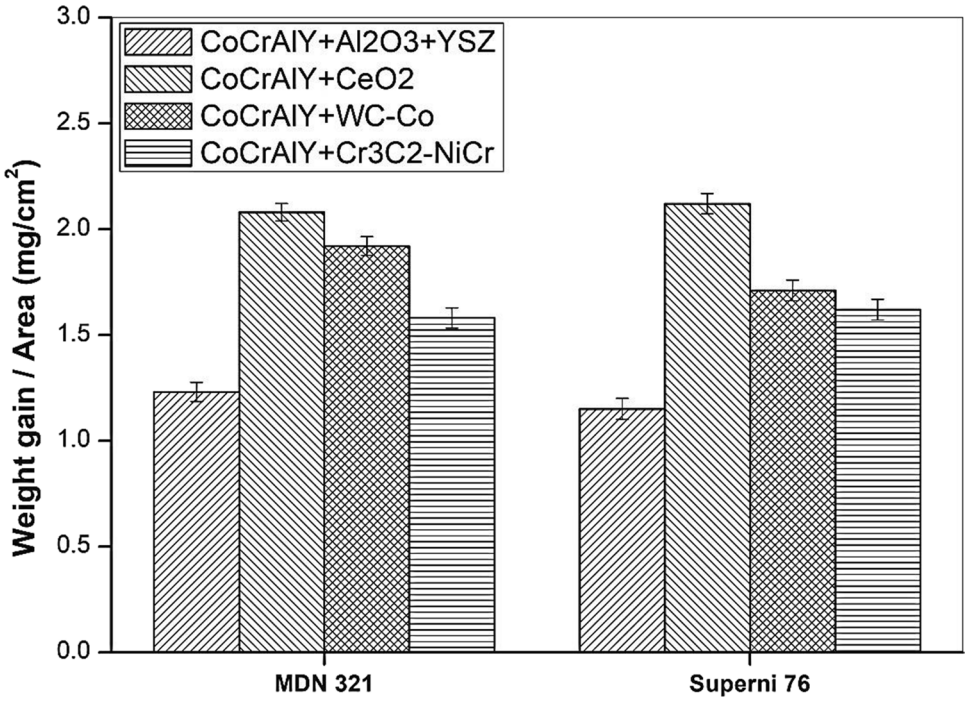

Fig. 5 Total weight gain (mg/cm^2) of uncoated and plasma-coated alloys subjected to oxidationWhen comparing the weight gain of the same coating on two distinct alloys, the coatings on two substrates with the larger total weight gain are evaluated. $CoCrAlY + Al_2O_3 + YSZ$ coatings gained roughly 28% less weight than $CoCrAlY + Cr_3C_2$-NiCr coatings, 34% less weight than CoCrAlY + WC–Co coatings, and 44% less weight than $CoCrAlY + CeO_2$ coatings. After oxidation, the main phases visible at the surface of coatings on two different alloys are identical

oxide scale thickness. Internal oxidation occurs in open pores during the earliest phases of oxidation for thermal sprayed metallic coatings, according to some research publications [20–22], corroborating the findings of our study. The major phases identified by XRD examination of an oxidised coated surface are Cr_2O_3, $CoCr_2O_4$, and $CoAl_2O_4$, which are thermodynamically stable and have a dense-packed globular shape.

CoCrAlY + Cr_3C_2-NiCr coating, on the other hand, comprises 36 (wt%) Cr, including Cr contained in Cr_3C_2-NiCr reinforcement. Because of the sophisticated Cr element in the coating, Cr is quickly transformed into Cr_2O_3 at the start. The presence of Cr_2O_3 as a dominant phase may be seen in the XRD results. Cr_2O_3 is a stable oxide that prevents oxidation and corrosion by limiting oxygen transport inward below 800 °C. Cr_2O_3 will change to CrO_3 at this temperature, which is a volatile oxide that is not suited for oxidation protection at higher temperatures [19]. The spinel oxides $CoCr_2O_4$ and $NiCr_2O_4$ are the predominant and minor phases in XRD analysis, respectively. $CoCr_2O_4$ and $NiCr_2O_4$ spinel oxides are formed via the nucleation of CoO-Cr_2O_3 and NiO-Cr_2O_3.

The active coating components namely Co, Cr, Al, and W have been oxidised to form CoO, Cr_2O_3, Al_2O_3, and WO_3 with respect to CoCrAlY + WC–Co coating. $CoWO_4$ as a strong phase with Cr_2O_3 and $CoCr_2O_4$ creates a thick, non-porous oxide scale with future oxidation cycles, providing resistance to oxidation. Similarly, during oxidation tests of W-based coatings, several researchers [23–25] found the occurrence of Cr_2O_3, $CoWO_4$, and $CoCr_2O_4$ as a strong phase. WO_3 is viewed as a porous structure that allows oxygen to diffuse inward until it converts into $CoWO_4$.

The oxidation of active components Al, Co, and Cr results in the production of oxide scale on the coated surface in the case of CoCrAlY + CeO_2 coating. Ce ions restrict outward diffusion of Co due to the segregation of CeO_2 at the grain boundaries of the oxide scale, and oxide scale growth is mainly controlled by inward diffusion of oxygen. CeO_2 segregation, on the other hand, occurs slowly, resulting in greater weight gain and cracks.

4 Conclusion

- CoCrAlY + Al_2O_3 + YSZ coatings have higher oxidation resistance than other coatings. Based on thermogravimetric data, the relative oxidation resistance of the various coatings is arranged in the following order.

$$\mathrm{CoCrAlY} + \mathrm{Al_2O_3} + \mathrm{YSZ} > \mathrm{CoCrAlY} + \mathrm{Cr_3C_2} - \mathrm{NiCr} > \mathrm{CoCrAlY} + \mathrm{WC} - \mathrm{Co} > \mathrm{CoCrAlY} + \mathrm{CeO_2}$$

- Slow-scale growth kinetics during oxidation was caused by an oxide layer of Al_2O_3, Cr_2O_3, and $CoCr_2O_4$ covering the outermost surface of CoCrAlY + Al_2O_3 + YSZ coatings. By selectively oxidising Al and Cr at the cobalt-rich splat boundary, air cannot penetrate the coating through pores or voids, keeping the oxidation rate constant.
- Because the CoCrAlY + Cr_3C_2-NiCr coating has a greater Cr concentration than the other coatings, Cr_2O_3 was formed quickly during the initial phases of oxidation. Cr_2O_3 with spinal oxides of $CoCr_2O_4$ and $NiCr_2O_4$ may hinder the inward passage of oxygen, lowering the rate of oxidation.
- The increased weight gain of CoCrAlY + WC–Co coating was due to the quicker oxidation of W into WO_3, which appears as a porous structure that enables oxygen to permeate until it transforms into $CoWO_4$. As a result of several oxidation cycles, thick, non-porous oxide scale made of Cr_2O_3, CoO, and Al_2O_3 was produced, which offered oxidation resistance.

Declarations

Conflict of interest The authors declare no competing interests.

References

1. Amaya C, Aperador W, Caicedo JC, Espinoza-Beltrán FJ, Muñoz-Saldaña J, Zambrano G, Prieto P (2009) Corrosion study of alumina/yttria-stabilized zirconia (Al_2O_3/YSZ) nanostructured thermal barrier coatings (tbc) exposed to high temperature treatment. Corros Sci 51(12):2994–2999
2. Prasad CD, Joladarashi S, Ramesh MR, Srinath MS, Channabasappa BH (2020) Comparison of high temperature wear behavior of microwave assisted HVOF sprayed CoMoCrSi-WC-CrC-Ni/WC-12Co composite coatings. Silicon, Springer 12:3027–3045. https://doi.org/10.1007/s12633-020-00398-1
3. Prasad CD, Joladarashi S, Ramesh MR, Srinath MS, Channabasappa BH (2019) Effect of microwave heating on microstructure and elevated temperature adhesive wear behavior of HVOF deposited CoMoCrSi-Cr3C2 composite coating. Surf Coat Technol Elsev Sci 374:291–304. https://doi.org/10.1016/j.surfcoat.2019.05.056
4. Madhusudana Reddy G, Durga Prasad C, Shetty G, Ramesh MR, Nageswara Rao T, Patil P (2022) High temperature oxidation behavior of plasma sprayed NiCrAlY/TiO_2 & NiCrAlY /Cr_2O_3/YSZ coatings on titanium alloy. Welding in the World. https://doi.org/10.1007/s40194-022-01268-7
5. Naik T, Mahantayya Mathapathi C, Prasad D, Nithin HS, Ramesh MR (2022) Effect of laser post treatment on microstructural and sliding wear behavior of HVOF sprayed NiCrC and NiCrSi coatings. Surf Rev Lett 29(1):225000. https://doi.org/10.1142/S0218625X2250007X
6. Prasad CD, Joladarashi S, Ramesh MR, Srinath MS, Channabasappa BH (2018) Influence of microwave hybrid heating on the sliding wear behaviour of HVOF sprayed CoMoCrSi coating. Mater Res Express 5:086519. https://doi.org/10.1088/2053-1591/aad44e.

7. Reddy MS, Durga Prasad C, Pradeep Patil MR, Ramesh NR (2021) Hot corrosion behavior of plasma sprayed NiCrAlY/TiO_2 and NiCrAlY/Cr_2O_3/YSZ cermets coatings on alloy steel. Surfaces Interfaces 22:100810. https://doi.org/10.1016/j.surfin.2020.100810.
8. James AW, Rajagopalan S (2014) "Gas turbines: operating conditions, components and material requirements." Structural alloys for power plants: operational challenges and high-temperature materials, 3–21.
9. Jafari M, Enayati MH, Salehi M, Nahvi SM, Han JC, Park C (2016) High temperature oxidation behavior of micro/nano-structured WC-Co coatings deposited from Ni-coated powders using high velocity oxygen fuel spraying. Surf Coat Technol 302:426–437
10. Nithin HS, Desai V, Ramesh MR (2017) "Elevated temperature solid particle erosion performance of plasma-sprayed co-based composite coatings with additions of Al2O3 and CeO2''. J Materials Eng Performance 26(11):5251–5261
11. Nithin HS, Desai V, Ramesh MR (2018) Elevated temperature solid particle erosion behaviour of carbide reinforced CoCrAlY composite coatings. Materials Res Express 5(6):066529
12. Ramesh MR, Prakash S, Nath SK, Kumar P, Venkataraman B (2010) Solid particle erosion of HVOF sprayed WC-Co/NiCrFeSiB coatings. Wear 269(3–4):197–205
13. Seo D, Ogawa K, Suzuki Y, Ichimura K, Shoji T, Murata S (2008) Comparative study on oxidation behavior of selected MCrAlY coatings by elemental concentration profile analysis. Appl Surf Sci 255:2581–2590
14. Sidhu BS, Prakash S (2006a) Performance of NiCrAlY, Ni-Cr, Stellite-6 and Ni_3Al coatings in Na_2SO_4-60% V_2O_5 environment at 900 °C under cyclic conditions. Surf Coat Technol 201(3–4):1643–1654
15. Hatami M, Naeimi F, Shamanian M, Tahari M (2018) High-temperature oxidation behavior of nano-structured CoNiCrAlY–YSZ coatings produced by HVOF thermal spray technique. Oxid Met 90(1):153–167
16. Ghadami F, Aghdam ASR, Ghadami S (2020) Preparation, characterization and oxidation behavior of CeO_2-gradient NiCrAlY coatings applied by HVOF thermal spraying process. Ceram Int 46(12):20500–20509
17. Hang Z, Xi N, Liu Y, Liu Y, Chen H (2018) High-temperature oxidation behavior of HVOF-sprayed rare earth-modified WC–12Co coating. Rare Met 1–8
18. Yao H, Jiang C, Bao Z, Zhu S, Wang F (2019) Preparation and oxidation performance of a NiCoCrAlYSiHf+NiAl composite coating deposited by arc ion plating and magnetron sputtering techniques. J Mater Eng Perform 28(2):1019–1029
19. Shi P, Wang W, Wan S, Gao Q, Sun H, Feng X, Wang Q (2021) Tribological performance and high temperature oxidation behaviour of thermal sprayed Ni-and NiCrAlY-based composite coatings. Surf Coat Technol 405:126615
20. Reddy MG, Prasad CD, Shetty G, Ramesh MR, Rao NT, Patil P (2021) High Temperature Oxidation Studies of Plasma Sprayed NiCrAlY/TiO2 & NiCrAlY /Cr2O3/YSZ Cermet Composite Coatings on MDN-420 Special Steel Alloy. Metallograph Microstruct Analy 10:642–651. https://doi.org/10.1007/s13632-021-00784-0
21. Singh H, Kaur M, Prakash S (2016) High-temperature exposure studies of HVOF-sprayed Cr_3C_2-25 (NiCr)/(WC-Co) coating. J Therm Spray Technol 25(6):1192–1207
22. Reddy GMS, Prasad CD, Shetty G, Ramesh MR, Rao NT, Patil P (2022) Investigation of thermally sprayed NiCrAlY/TiO2 and NiCrAlY/Cr2O3/YSZ cermet composite coatings on titanium alloys. Eng Res Exp 4:025049. https://doi.org/10.1088/2631-8695/ac7946
23. Reddy MG, Prasad CD, Patil P, Kakur N, Ramesh MR (2022) Elevated temperature erosion performance of plasma sprayed NiCrAlY/TiO2 coating on MDN 420 steel substrate. Surf Topograph Metrol Propert 10:025010. https://doi.org/10.1088/2051-672X/ac6a6e
24. Zhu L, Zhu S, Wang F (2013) Applied surface science hot corrosion behaviour of a Ni+CrAlYSiN composite coating in Na_2SO_4–25wt.% NaCl melt. Appl Surf Sci 268:103–110
25. Praveen AS, Arjunan A (2022) High-temperature oxidation and erosion of HVOF sprayed NiCrSiB/Al_2O_3 and NiCrSiB/WCCo coatings. Appl Surface Sci Adv 7:100191